AMERICAN ACADEMY OF OPHTHALMOLOGY®

Relationship Between Retinal Layer Thickness and Genetic Susceptibility to Age-Related Macular Degeneration in Asian Populations

Kai Xiong Cheong, FRCOphth,[1] *Hengtong Li, MSc,*[1] *Yih Chung Tham, PhD,*[1,2,3] *Kelvin Yi Chong Teo, PhD,*[1,2] *Anna Cheng Sim Tan, FRCSEd (Ophth),*[1,2] *Leopold Schmetterer, PhD,*[1,2] *Tien Yin Wong, PhD,*[4] *Chui Ming Gemmy Cheung, FRCOphth,*[1,2] *Ching-Yu Cheng, PhD,*[1,2,3] *Qiao Fan, PhD*[2,5]

Purpose: For OCT retinal thickness measurements to be used as a prodromal age-related macular degeneration (AMD) risk marker, the 3-dimensional (3D) topographic variation of the relationship between genetic susceptibility to AMD and retinal thickness needs to be assessed. We aimed to evaluate individual retinal layer thickness changes and topography at the macula that are associated with AMD genetic susceptibility.

Design: Genetic association study.

Participants: A total of 1579 healthy participants (782 Chinese, 353 Malays, and 444 Indians) from the multiethnic Singapore Epidemiology of Eye Diseases study were included.

Methods: Spectral-domain OCT and automatic segmentation of individual retinal layers were performed to produce 10 retinal layer thickness measurements at each ETDRS subfield, producing 3D topographic information. Age-related macular degeneration genetic susceptibility was represented via single nucleotide polymorphisms (SNPs) and aggregated via whole genome (overall) and pathway-specific age-related macular degeneration polygenic risk score (PRS_{AMD}).

Main Outcome Measures: Associations of individual SNPs, overall PRS_{AMD}, and pathway-specific PRS_{AMD} with retinal thickness were analyzed by individual retinal layer and ETDRS subfield.

Results: *CFH* rs10922109, *ARMS2-HTRA1* rs3750846, and *LIPC* rs2043085 were the top AMD susceptibility SNPs associated with retinal thickness of individual layers ($P < 1.67 \times 10^{-3}$), all at the central subfield. The overall PRS_{AMD} was most associated with thinner L9 (outer segment photoreceptor/retinal pigment epithelium complex) thickness at the central subfield ($\beta = -0.63$ μm; $P = 5.45 \times 10^{-9}$). Pathway-specific PRS_{AMD} for the complement cascade ($\beta = -0.53$ μm; $P = 9.42 \times 10^{-7}$) and lipoprotein metabolism ($\beta = -0.05$ μm; $P = 0.0061$) were associated with thinner photoreceptor layers (L9 and L7 [photoreceptor inner/outer segments], respectively) at the central subfield. The mean PRS_{AMD} score was larger among Indians compared with that of the Chinese and had the thinnest thickness at the L9 central subfield ($\beta = -1.00$ μm; $P = 2.91 \times 10^{-7}$; $R^2 = 5.5\%$). Associations at other retinal layers and ETDRS regions were more heterogeneous.

Conclusions: Overall genetic susceptibility to AMD and the aggregate effects of the complement cascade and lipoprotein metabolism pathway are associated most significantly with L7 and L9 photoreceptor thinning at the central macula in healthy individuals. Photoreceptor thinning has potential to be a prodromal AMD risk marker, and topographic variation should be considered.

Financial Disclosure(s): Proprietary or commercial disclosure may be found in the Footnotes and Disclosures at the end of this article. *Ophthalmology Science 2023;3:100396* © *2023 by the American Academy of Ophthalmology. This is an open access article under the CC BY-NC-ND license (http://creativecommons.org/licenses/by-nc-nd/4.0/).*

Supplemental material available at www.ophthalmologyscience.org.

Age-related macular degeneration (AMD) is a major cause of severe and irreversible visual impairment globally.[1–3] Studies have suggested that the thickness of individual retinal layers is a useful biomarker of future AMD risk. Photoreceptor loss and retinal pigment epithelium (RPE) thickening are independently associated with AMD.[4–6] Photoreceptor length is decreased in AMD, likely reflecting oxidative stress, leading to an imbalance in regeneration and phagocytosis.[7,8] Retinal pigment epithelium thickening is likely due to drusen accumulation and extracellular matrix

https://doi.org/10.1016/j.xops.2023.100396
ISSN 2666-9145/23

alterations, with resultant dysfunction and apoptosis.[7,8] Retinal pigment epithelium degeneration, in turn, causes photoreceptor dysfunction.

Using a genetic approach to identify associations of individual retinal layer thickness with AMD genetic susceptibility will provide insights into the role of AMD biomarkers at an early stage of disease development. A comprehensive genome-wide association study (GWAS) for AMD that was performed on a population of European ancestry identified 34 genetic loci, including those in *CFH* and *ARMS2-HTRA1* genes.[9] Our previous study on an East Asian population confirmed previously identified AMD susceptibility single nucleotide polymorphisms (SNPs).[10] A UK Biobank study has reported that a thinner inner-segment outer segment RPE layer was significantly associated with a genetic risk score that comprised 33 AMD-related genetic variants.[5] A separate UK Biobank study reported that whole-genome age-related macular degeneration polygenic risk score (PRS_{AMD}) was associated with photoreceptor segment thinning and had a U-shaped association with the RPE and Bruch's membrane thickness.[6]

However, although reported changes in the outer retina in AMD are relatively consistent, those in the inner retinal layers are less so. Fewer and smaller studies have described thinning of the retinal nerve fiber layer (RNFL), ganglion cell layer (GCL), and inner plexiform layer (IPL) in AMD.[11,12] Additionally, previous studies that assessed the associations between AMD genetic susceptibility and retinal thickness have focused on the outer retina or used overall mean measurements of the individual retinal layers. Furthermore, most of these studies were performed on European populations.

We propose that the 3-dimensional (3D) topographic variation of the relationship between AMD genetic susceptibility and retinal thickness is currently not well understood enough for OCT retinal thickness measurements to be used as a prodromal AMD risk marker. It is important to assess the macula by individual retinal layers and use an ETDRS grid to characterize the 3D topography. This is because the retina is a complex 3D structure. For example, cone density peaks at the fovea and decreases with eccentricity.[13] In AMD, druse-associated progression risk is concentrated in the central macula, specifically in the central subfield and inner ring of the ETDRS grid in population-based studies.[14]

In a multiethnic Asian population-based study, we aimed to assess the individual retinal thickness of all 10 retinal layers, their 3D topographic distributions, and their associations with AMD genetic susceptibility variants and PRS_{AMD}.

Methods

Study Population

This study utilized data from the Singapore Epidemiology of Eye Diseases (SEED) study, which comprises prospective population-based cohort studies of Chinese, Malays, and Indians in Singapore. The study design and methodology were described previously.[15–17] Briefly, an age-stratified random sampling strategy was adopted in each ethnic group to recruit adults of age 40–80 years to participate in the study. A total of 1579 healthy participants (782 Chinese, 353 Malays, and 444 Indians) with both retinal thickness and genotype data available in SEED, and without AMD and other ocular diseases, were included in this study. The study adhered to the tenets of the Declaration of Helsinki. Ethics approval was obtained from the Institutional Review Board of the Singapore Eye Research Institute. Written informed consent was obtained from all participants.

Phenotyping

Participants underwent Cirrus spectral-domain OCT (Carl Zeiss Meditec, Inc) imaging after pupil dilation to acquire 200 × 200 macular and optic disc cube scans in each eye. The automatic analysis of retinal thickness was described previously.[18–20] The OCT images were imported into the automatic OCT layer segmentation algorithm (Retinal Image Analysis Lab, Iowa Institute for Biomedical Imaging). The retina was segmented into 10 constituent layers (L), comprising the L1: RNFL; L2: GCL; L3: IPL; L4: inner nuclear layer; L5: outer plexiform layer; L6: outer nuclear layer; L7: photoreceptor inner/outer segments; L8: inner/outer segment junction to inner boundary of outer segment photoreceptor/RPE complex; L9: outer segment photoreceptor/RPE complex; and L10: RPE. ETDRS grid thickness maps were generated. See Figure 1 for an illustration.

Genotyping

Genotyping of whole blood samples obtained from the participants was performed using Illumina Human OmniExpress or Human Hap610-Quad BeadChips (Illumina, Inc). The detailed data quality control was described previously.[21,22] Briefly, a first round of SNP quality control was performed to obtain a cleaned set of genotypes. Single nucleotide polymorphisms flagged with high missingness (5%), with a gross departure from Hardy–Weinberg equilibrium ($P < 10^{-6}$), of minor allele frequency <1%, and those that were monomorphic were excluded. Samples with low call rates of <95%, excessive heterogeneity, cryptic relatedness, and gender discrepancies were also excluded.

To identify discordant ethnic memberships from self-reported ethnicity, we conducted principal component analyses for each ethnic group. We identified outliers within each population using plots of up to 5 principal components. The distinct clustering of the 1579 participants on the principal component analysis plot, specifically along the first and second principal components, indicates that the populations are distinguishable (Fig S2).

The array genotypes were then prephased using SHAPEIT version 2[23] and imputed using the 1000 Genomes Project data as reference panels (build 37, hg19, phase 3 release; March 2012)[24] with the Michigan imputation server (Minimac3).[25] Imputed genotypes were called with posterior probability exceeding a threshold of 0.7. The coordinates and variant identifiers were based on the National Center for Biotechnology Information B37 (hg19) genome build. The functional annotation and gene mapping were performed using ANNOVAR (version 2018; April 2016).[26]

PRS_{AMD}

The overall PRS_{AMD} of whole genome was constructed with SEED data using the SNP scoring function in PLINK2.[27] We derived PRS_{AMD} using beta effects as weights from the Genetics of AMD in Asians (GAMA) Consortium.[9,28] Independent genetic variants were identified with the "clumping and thresholding"

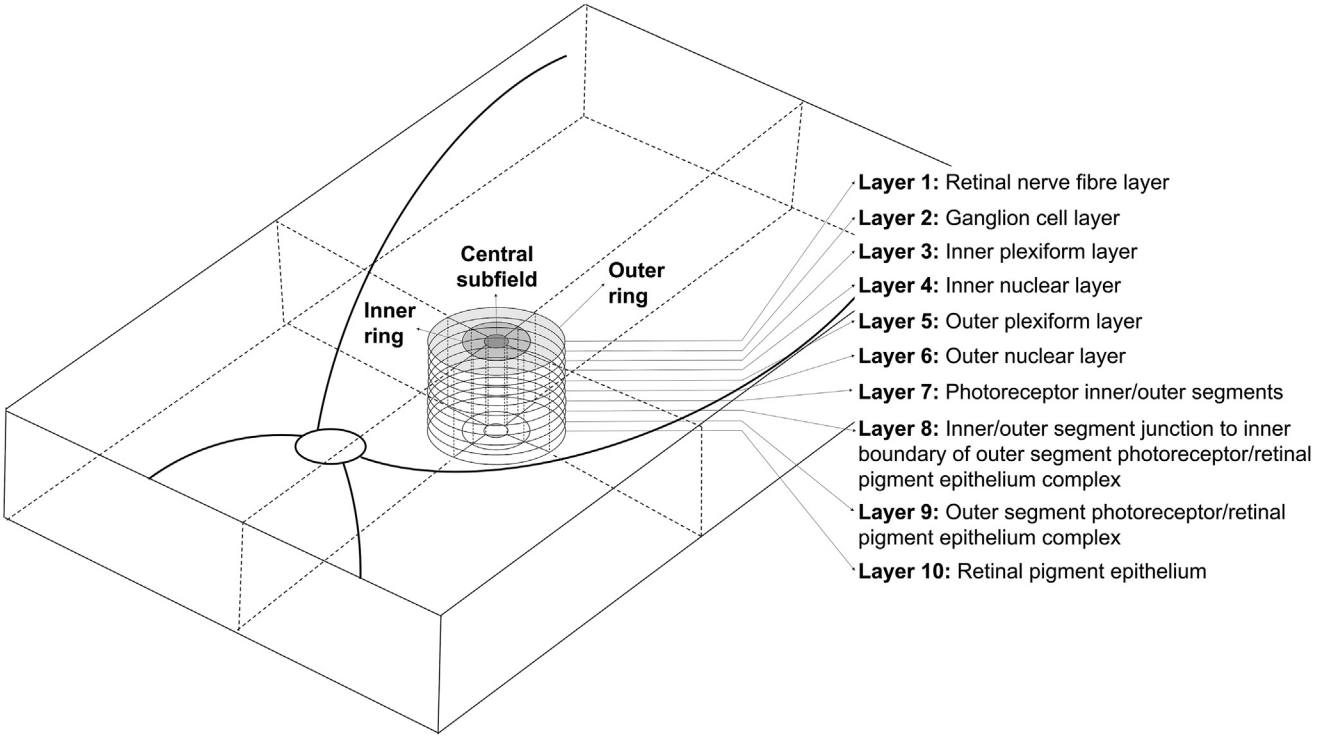

Figure 1. Three-dimensional illustration of macular topography. The retina was segmented into 10 constituent layers. Thickness maps were generated, which provided mean macular thickness measurements for the 9 sectors of the ETDRS grid, which were combined to form 3 concentric regions, comprising the central subfield (1-mm diameter), inner ring (3-mm diameter), and outer ring (6-mm diameter).

approach, removing variants at linkage disequilibrium (LD) ($r^2 > 0.1$) within 500 kb of the index variant. We first estimated PRS_{AMD} R^2 and empirical P values for association with 30 retinal layer phenotypes in Chinese samples at a series of P-value thresholds of 1×10^{-2}, 1×10^{-3}, 1×10^{-4}, 1×10^{-5}, 1×10^{-6}, and 5×10^{-8} using the permutation procedure implemented in the PRSice-2 software.[29] The P-value cutoff at 1×10^{-4} was selected because it produced the largest number of retinal layer phenotypes in the Chinese cohort with a R^2 of 0.5% or 1% (Table S1). Therefore, a total of 255 variants were used to create PRS_{AMD}. We further generated PRS_{AMD} at a P value of 1×10^{-4} in the SEED data of the Chinese, Indian, and Malay populations separately using AMD risk alleles using the SNP scoring function in PLINK2.[27] Linkage disequilibrium reference panels were based on the population-specific genotype data from SEED participants. The proportion of variance in the retinal thickness that is attributed to a PRS_{AMD} was assessed by using the difference of R^2 between the full model (full linear regression model with PRS_{AMD})[30] and the null model (without PRS_{AMD}).[29]

To understand aggregate pathway-specific effects, we calculated pathway-specific PRS_{AMD} for the complement cascade, lipoprotein metabolism pathway, and collagen pathway, using the index SNPs in each gene for the complement cascade (6 SNPs: *C3* rs2642198, *CFH* rs10922109, *C9* rs835191, *CFI* rs10033900, *CFB* rs429608, and *TMEM97-VTN* rs11080055), lipoprotein metabolism (5 SNPs: *APOE* rs769449, *CETP* rs5817082, *LIPC* rs2043085, *ABCA1* rs2740488, and *ABCA7* rs739884), and collagen pathway (7 SNPs: *COL15A1* rs1626340, *COL8A1* rs2315840, *LOXL2* rs13278062, *COL4A3* rs11884770, *COL4A4* rs56033528, *MMP9* rs1888235, and *PCOLCE* rs7803454).[9,28] PRS_{AMD} was the summation of the risk alleles weighted by the beta effects obtained from the GAMA GWAS summary statistics.[9,28]

Statistical Analysis

Association between AMD Susceptibility SNPs and Retinal Layer Thickness. For the associations between AMD susceptibility SNPs and retinal layer thickness, we included 33 SNPs studied in previous GWAS.[9,28] We required an imputation quality score of at least 0.7. We used alternative genome-wide significant SNPs that are in LD r^2 of at least 0.6 if the identified lead SNPs were missing. We tested the associations between hard call genotypes and each phenotype using the right eye adjusted for age, sex, spherical equivalent, and the first 5 principal components using individual level data. Analyses were conducted in PLINK2 under a linear regression model.[27] A total of 30 phenotypes were analyzed [10 retinal layers x 3 ETDRS subfields (central subfield, inner ring, and outer ring)]. The per-SNP meta-analyses were performed in Metal software with a weighted inverse-variance approach to obtain the combined effect estimates of individual SNPs.[31] For single variant analysis, significance was set at $P < 5.05 \times 10^{-5}$ [original alpha 0.05/(33 SNPs $\times$ 10 retinal layers $\times$ 3 ETDRS subfields)]. Nominal significance was set at $P < 1.67 \times 10^{-3}$ [original alpha 0.05/(10 retinal layers $\times$ 3 ETDRS subfields)]. Marginal significance was set at $P < 0.05$.

Association between PRS_{AMD} and Retinal Layer Thickness. The associations of the overall and pathway-specific PRS_{AMD} with the thickness of each retinal layer at each ETDRS subfield were assessed using linear regression models that were adjusted for age, sex, spherical equivalent, and the top 5 principal components. The model without adjusting for spherical equivalent yielded similar results. Inverse-variance-based meta-analysis was adopted to calculate an overall genetic effect of PRS_{AMD} among the 3 ethnic groups. A total of 30 phenotypes were analyzed (10 retinal layers $\times$ 3 ETDRS subfields), and the association estimates

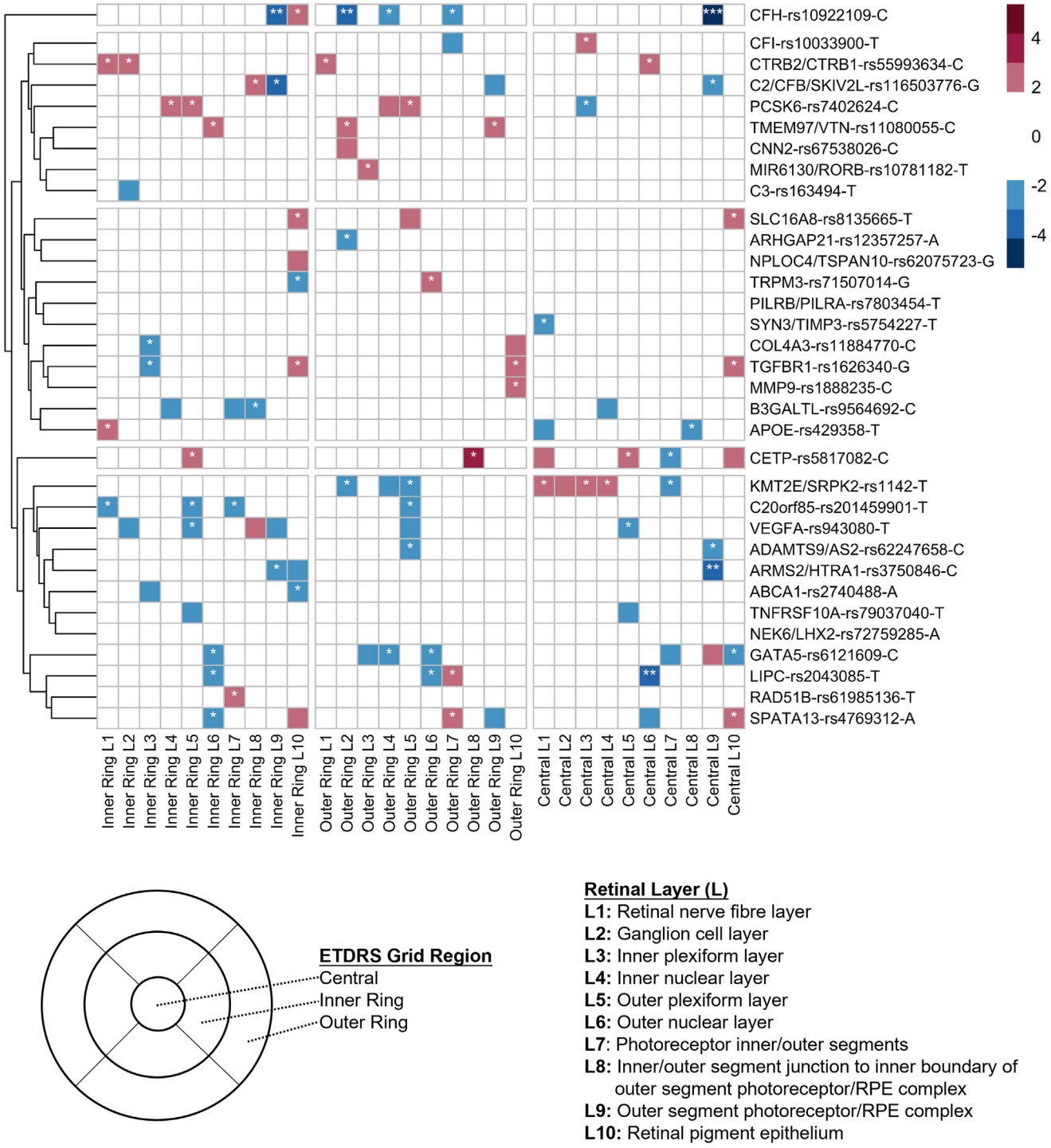

Figure 3. Heat map of the associations of age-related macular degeneration susceptibility single nucleotide polymorphisms (SNPs) with retinal thickness. The associations of 33 SNPs with the mean retinal thickness of all 10 retinal layers and in the central subfield, inner ring, and outer ring of the ETDRS grid were assessed. Individual level data from the Singapore Epidemiology of Eye Diseases study were used. Linear regression models that were adjusted for age, sex, spherical equivalent, and the first 5 principal components. The y-axis displays the gene, reference SNP (RS) identifier number, and effect allele for each SNP. The x-axis displays all 10 retinal layers in the central subfield, inner ring, and outer ring of the ETDRS grid. Z-scores were used for the heat map. Positive values are displayed in red, and negative values are displayed in blue. In each cell, *** represents a significance level of $P < 5.05 \times 10^{-5}$, ** represents a nominal significance at $P < 1.67 \times 10^{-3}$, and * represents marginal significance at $P < 0.05$. Nonsignificant associations were not annotated with any asterisk symbols. RPE = retinal pigment epithelium.

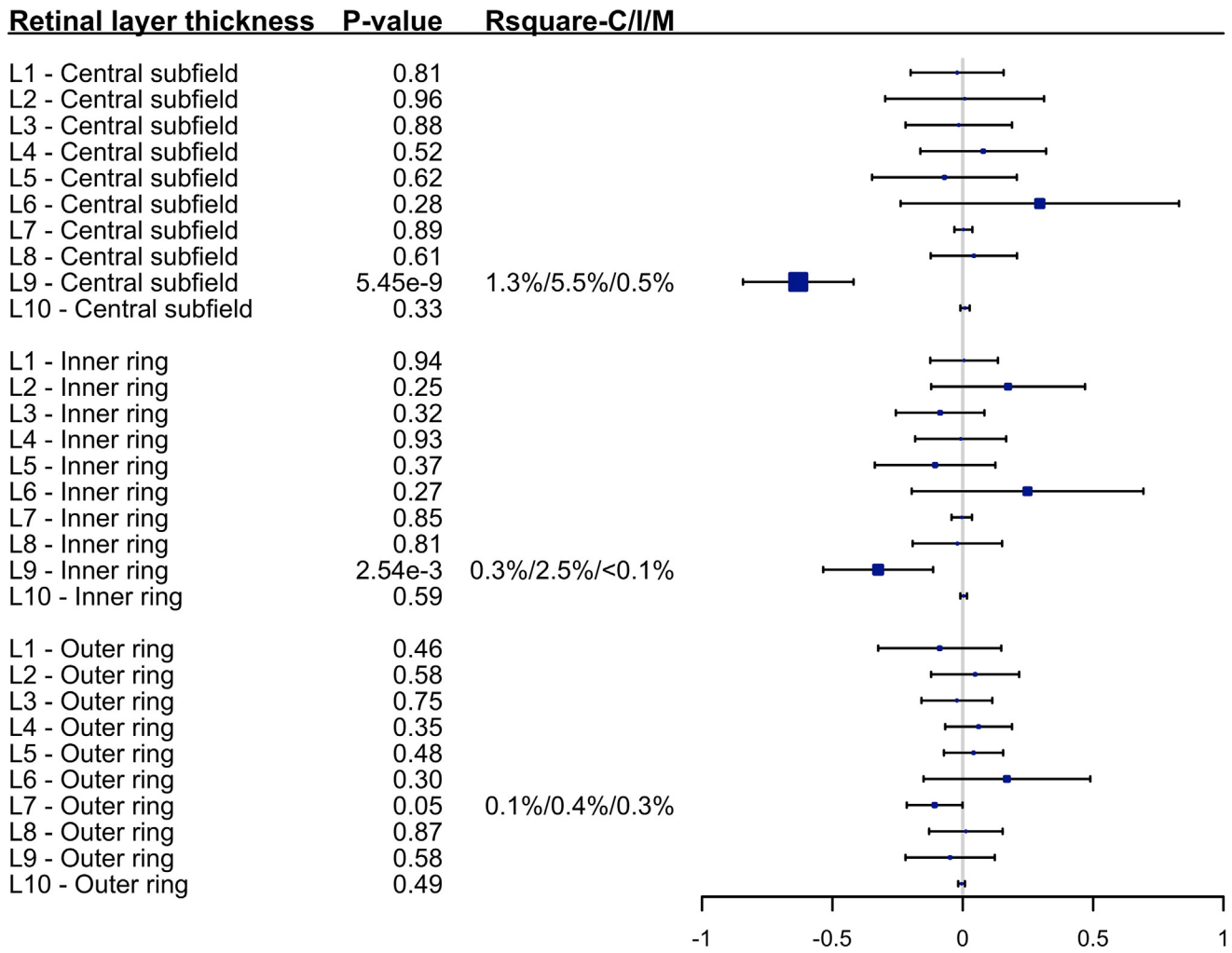

Figure 4. Forest plot of associations of whole-genome age-related macular degeneration polygenic risk score (PRS_{AMD}) with retinal thickness. The forest plot demonstrates the respective associations between whole-genome PRS_{AMD} with L1 to L10 retinal thickness at central, inner ring, and outer ring of the ETDRS grid. The overall PRS_{AMD} that aggregated a collection of independent single nucleotide polymorphisms at a *P*-value threshold of 1×10^{-4} was most associated with the thinner photoreceptor (L9) retinal thickness at the central subfield ($\beta = -0.63$ μm, $P = 5.450 \times 10^{-9}$).

were presented on the forest plot. Also, for the photoreceptor layers (L7 to L9), we analyzed individual subfields, that is, superior, inferior, nasal, and temporal subfields of each ring, and the association estimates were presented on radar plots. Interstudy/population heterogeneity (I^2) was assessed. The R^2 attributed to PRS_{AMD} for each population was estimated.

PRS_{AMD} among Ethnic Groups. The population-specific associations of both the overall and pathway-specific PRS_{AMD} were assessed for the Chinese, Malay, and Indian populations. The differences in the mean PRS_{AMD} between the 2 ethnic groups were tested using the 2-sample *t*-test. We tested the differences in beta effects for L9 central region between 2 ethnic groups (Indians vs. Chinese), assuming a normal distribution. Family-wise type-1 error was controlled at 0.05.

Results

A total of 1579 healthy participants (782 Chinese, 353 Malay, and 444 Indian participants) were studied. The mean age was 53.1 years, and 49.2% of the participants were female. Detailed information is found in Table S2.

Association of AMD Susceptible SNPs

Overall, the top AMD SNPs that were most significantly associated with retinal thickness were *CFH* rs10922109, *ARMS2-HTRA1* rs3750846, and *LIPC* rs2043085. The significant SNPs were associated with a thinner retina at the photoreceptor layers (L7 to L9) at the central subfield. In the inner and outer rings and the other retinal layers (L1 to L6), the associations were mostly marginal in significance and more heterogeneous, that is, associations with both thinner and thicker retinas. See Figure 3 for the heat smap of the associations for L7 to L9 by ETDRS grid region. See Table S3 for the full associations.

Photoreceptor Layers. At the central subfield for L7 to L9, 7 SNPs were associated with a thinner L9. The strongest

Table 4. Association of Polygenic Risk Score (PRS_{AMD}) with Photoceptor Layer (L7–L9) Thickness (μm)

	L7: Photoreceptor Inner/Outer Segments			L8: Inner/Outer Segment Junction to Inner Boundary of Outer Segment Photoreceptor/RPE Complex			L9: Outer Segment Photoreceptor/ RPE Complex (OPR)		
ETDRS Region	*Central Subfield*	*Inner Ring*	*Outer Ring*	*Central Subfield*	*Inner Ring*	*Outer Ring*	*Central Subfield*	*Inner Ring*	*Outer Ring*
Overall PRS_{AMD}									
Overall									
β	0.003	−0.004	−0.108	0.043	−0.021	0.012	−0.631	−0.325	−0.048
SE	0.018	0.020	0.055	0.085	0.088	0.072	0.108	0.108	0.087
P	0.886	0.852	**0.048**	0.613	0.814	0.868	**5.450×10^{-9}**	**0.003**	0.580
Pathway-specific PRS_{AMD}									
Complement Cascade									
β	−0.004	−0.015	−0.182	0.008	−0.036	3.000×10^{-4}	−0.526	−0.330	−0.019
SE	0.017	0.020	0.054	0.083	0.087	0.071	0.107	0.107	0.087
P	0.840	0.455	**0.001**	0.927	0.676	0.997	**9.420×10^{-7}**	**0.002**	0.831
Lipoprotein Metabolism									
β	−0.048	−0.048	−0.069	−0.101	−0.141	0.068	−0.014	0.081	−0.064
SE	0.017	0.019	0.054	0.083	0.087	0.071	0.108	0.107	0.087
P	**0.006**	**0.015**	0.201	0.227	0.103	0.340	0.900	0.452	0.462
Collagen Pathway									
β	−0.012	0.027	−0.009	0.063	−0.021	−0.131	−0.173	−0.123	0.066
SE	0.017	0.020	0.054	0.083	0.087	0.071	0.108	0.107	0.087
P	0.476	0.168	0.873	0.449	0.806	0.066	0.109	0.252	0.444

L = layer; PRS_{AMD} = age-related macular degeneration polygenic risk score; RPE = retinal pigment epithelium; SE = standard error.
β represents the change (μm) in the thickness of subfields for layer L7 to L9 per standard deviation increase in PRS_{AMD}.
The associations of overall PRS_{AMD} and pathway-specific PRS_{AMD} for all 10 retinal layer thickness, including in the central subfield, inner ring, and outer ring, are presented in Tables S5 and S6, respectively.
These associations have been adjusted for sex, age, spherical equivalent, and 5 principal components.
Associations that have at least a marginal significance of $P < 0.05$ are highlighted in bold.

association ($\beta = -0.88$ μm; $P = 8.66 \times 10^{-8}$) was observed at L9 with *CFH* rs10922109. Also, *ARMS2-HTRA1* rs3750846 displayed a nominal association ($\beta = -0.62$ μm; $P = 2.06 \times 10^{-4}$) with a thinner L9. Other SNPs showed marginal significance: *CETP* rs5817082, *ADAMTS9-AS2* rs62247658, *C2-CFB-SKIV2L* rs116503776, *KMT2E-SRPK2* rs1142, and *APOE* rs429358.

In the inner and outer rings, *CFH* rs10922109 C allele demonstrated significant association with a thinner retina in the inner ring ($\beta = -0.60$ μm; $P = 3.22 \times 10^{-4}$) and was the only SNP associated with thinner photoreceptor layers at all 3 regions of central subfield (L9), inner ring (L7), and outer ring (L9). The other significant SNPs showed marginal significance, including *ARMS2-HTRA1* rs3750846, *C2-CFB-SKIV2L* rs116503776, *B3GALTL* rs9564692, *RAD51B* rs61985136, *LIPC* rs2043085, *CETP* rs5817082, *TMEM97-VTN* rs11080055, *C20orf85* rs201459901, and *SPATA13* rs4769312.

RPE. For L10, the significant SNPs were *CFH* rs10922109, *TGFBR1* rs1626340, *ABCA1* rs2740488, *MMP9* rs1888235, *SLC16A8* rs8135665, *SPATA13* rs4769312, and *GATA5* rs6121609 ($P < 0.05$), but none remained significant after multiple testing correction. These AMD-risk alleles were mostly associated with a thicker RPE. Notably, *TGFBR1* rs1626340 G allele was the only variant associated with a thicker RPE at all 3 regions of the central subfield, inner ring, and outer ring.

Inner Retina. For L1 to L6, 2 SNPs showed significant associations: *CFH* rs10922109 with a thinner L2 ($\beta = -0.47$ μm; $P = 3.43 \times 10^{-4}$) and *LIPC* rs2043085 with a thicker L6 ($\beta = 1.32$ μm; $P = 6.60 \times 10^{-4}$). The remaining SNPs showed marginal associations.

Associations of Overall PRS_{AMD}

Figure 4 displays the forest plot of the associations of the overall PRS_{AMD} with L1 to L10 thickness by ETDRS grid region. We assessed the associations at the central subfield, inner ring, and outer ring of each retinal layer. The strongest association was found at the central subfield of the L9 ($P = 5.450 \times 10^{-9}$; R^2 range: 0.5%–5.5%). There were marginal associations at L9 inner ring ($P = 2.542 \times 10^{-3}$; R^2 range: 0.1%–2.5%) and L7 outer ring ($P = 0.4821$; R^2 range: 0.1%–0.4%).

For L9 and L7, one standard deviation increase in overall PRS_{AMD} was associated with the reduction of retinal thickness at the L9 central subfield [$\beta = -0.63$ μm, standard error (SE) = 0.11], inner ring ($\beta = -0.32$ μm, SE = 0.11), and L7 outer ring ($\beta = -0.11$, SE = 0.05; Table 4). There was substantial interpopulation heterogeneity ($I^2 = 65.7\%$) for the strongest association at L9 central subfield (Table S5).

We further compared the effects for ethnic-specific associations. The Indian population demonstrated the thinnest retinal thickness in the central subfield at L9 per standard deviation increase in PRS_{AMD} ($\beta = -1.00$ μm; $P = 2.91 \times 10^{-7}$) compared with the Chinese ($\beta = -0.52$ μm; $P = 1.11 \times 10^{-3}$), $P = 0.052$ (Fig 5A). The top versus

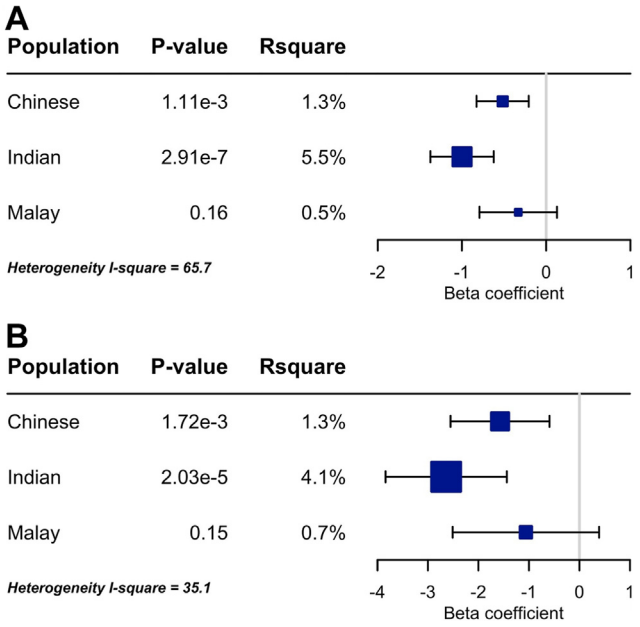

Figure 5. Ethnic-specific differences in associations between overall age-related macular degeneration polygenic risk score (PRS_{AMD}) and retinal thickness. **A,** For ethnic-specific associations, the Indian population demonstrated a nominally greater decrease in retinal thickness in the central subfield at L9 per unit increase in the overall PRS_{AMD} ($\beta = -1.00$ μm; $P = 2.91 \times 10^{-7}$) compared with the Chinese ($\beta = -0.52$ μm; $P = 1.11 \times 10^{-3}$). **B,** The top vs. bottom 20% of PRS_{AMD} were also examined. Although there was a trend showing that Indian samples had larger beta effects compared to Chinese samples ($\beta = -2.64$ μm; $P = 2.03 \times 10^{-5}$ vs. $\beta = -1.57$ μm; $P = 1.72 \times 10^{-3}$, respectively), the difference was not significant ($P = 0.177$).

the bottom 20% of PRS_{AMD} was also examined. Although there was a trend showing that Indian samples had larger beta effects compared with the Chinese samples ($\beta = -2.64$ μm; $P = 2.03 \times 10^{-5}$ vs. $\beta = -1.57$ μm; $P = 1.72 \times 10^{-3}$, respectively), the difference was nonsignificant ($P = 0.177$), likely due to the small sample size (Fig 5B). Furthermore, there was a mean shift of the overall PRS_{AMD} distribution of the Indians away from that of the Chinese (PRS_{AMD} mean of 71.34 vs. 74.55; $P < 2.2 \times 10^{-16}$) (Fig 6). One potential reason could be that the AMD-risk allele is more common in Indians compared with that in the Chinese population.

In addition, for L7 to L9, we proceeded to examine the individual subfields and observed similar associations at the superior, nasal, and temporal subfields of the inner ring at L9 (P range: 0.001−0.007) of the inferior and temporal subfields of the outer ring at L7 (P range: 0.010−0.033). See Supplementary Appendix 1 for the radar plots of the associations of the overall PRS_{AMD} with L7 to L9 thickness in individual ETDRS subfields.

Associations of Pathway-Specific PRS_{AMD}

The pathway-specific PRS_{AMD} for the complement cascade was also most associated with L9 retinal thickness at the central subfield ($\beta = -0.53$ μm; SE = 0.11; Table 4 and Table S6). There were also significant associations with the thinner mean retinal thickness of the inner ring and of all subfields of the inner ring at L9, and with the outer ring thickness and of all subfields of the outer ring at L7 (P range: 4.27×10^{-4}−0.02). See Supplementary Appendix 2 for the radar plots of the associations of the pathway-specific PRS_{AMD} with L7 to L9 thickness in individual ETDRS subfields.

The pathway-specific PRS_{AMD} for the lipoprotein metabolism pathway was most associated with the L7 retinal thickness at the central subfield ($\beta = -0.05$ μm; SE = 0.02). For the subfields, marginal significant associations were noted at the superior, inferior, and temporal subfields of the inner ring at L7 and with the temporal subfields of the inner ring at L8. No significant associations were observed for the collagen pathway.

Discussion

Through the analysis of retinal thickness by individual layers and ETDRS subfields, we established that overall genetic susceptibility to AMD and the aggregate effects of the complement cascade and lipoprotein metabolism pathway are associated most significantly with photoreceptor thinning, particularly at the L7 and L9 central macula in healthy individuals.

This study has assessed otherwise healthy individuals, albeit with decreased retinal thickness. Thus, L7 to L9 photoreceptor thinning indicates genetic susceptibility to AMD and is an early biomarker. This concurs with the UK Biobank studies[5,6] and supports studies that have suggested pathophysiological roles of complement factor and lipoprotein metabolism pathway dysregulation in AMD.[32,33] In contrast, the nonsignificant signals associated with the collagen pathway that are involved in extracellular matrix remodeling and fibrosis in AMD suggest that there are no strong associations with retinal thickness in healthy individuals.

The associations of the complement factor and lipoprotein metabolism pathways with thinner photoreceptor layers cohere with what we understand so far regarding the roles that aging, lipid accumulation, and cholesterol play in AMD development, with a resultant deregulated inflammatory host response that involves the complement pathway.[34−38] These have a strong genetic basis. Dysregulation in *CFH* and *ARMS2-HTRA1* is associated with systemic complement activation and oxidative stress.[32] *CFH* is expressed at high levels in the choroidal endothelial cells and the RPE, where it inhibits complement activation and prevents cellular damage, like systemic *CFH*.[36] The *ARMS2* protein is present in the choroidal extracellular matrix and may play a role in the pathogenesis of AMD via oxidative stress.[36]

In our study, the pathway-specific PRS_{AMD} for lipoprotein metabolism was associated with thinner photoreceptor layers. The age-dependent lipid accumulation in the RPE-Bruch's membrane contributes to the accumulation of drusen, basal linear and laminar deposits, and subretinal drusenoid deposits in the subretinal, sub-RPE,

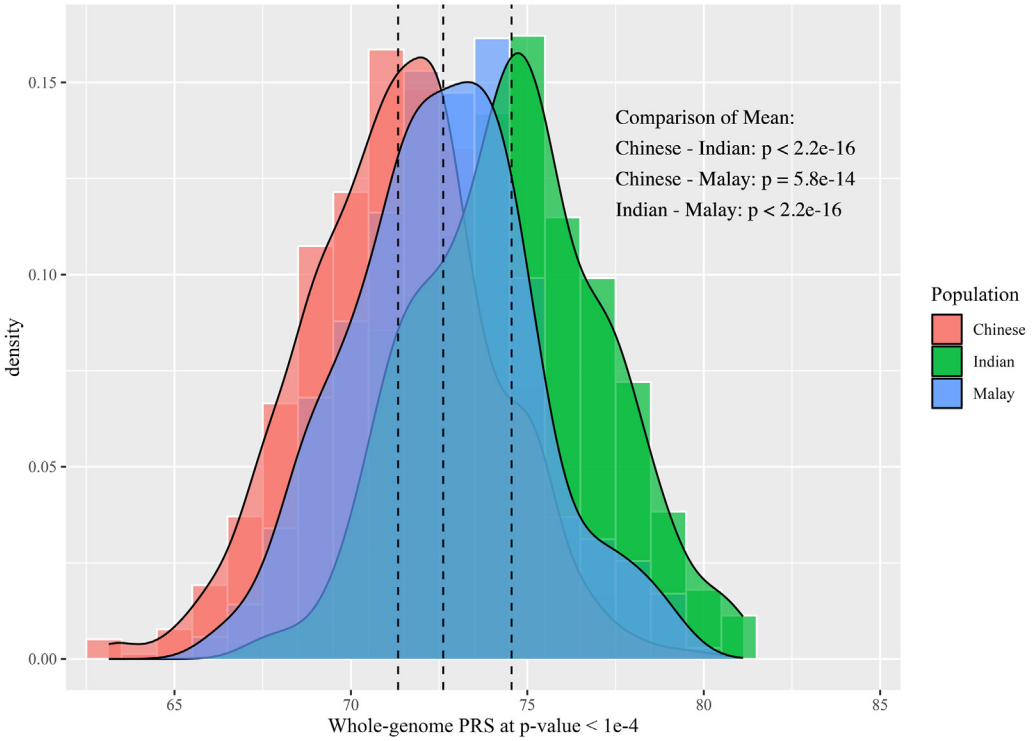

Figure 6. Histogram of overall age-related macular degeneration polygenic risk score (PRS) distribution by population. The histogram shows the respective whole-genome PRS distributions at a threshold *P* value of 1×10^{-4} of the Chinese (in red), Malay (in blue), and Indian (in green) populations. The population mean is indicated with vertical dash lines. The distributions of PRS are consistent with a normal distribution.

Bruch's membrane, and intercapillary pillar spaces.[32–34] Some studies have hypothesized that impaired recycling in the photoreceptors due to photoreceptor degeneration or thinning could increase the cholesterol load on the RPE and thereby increase lipid and protein excretion from the basal RPE, leading to drusen development.[6] In the reverse direction, other studies have hypothesized that it is hypoxia in the photoreceptor layer as a result of drusen development that leads to photoreceptor degeneration.[6]

Although positive or bimodal associations of RPE thickness with AMD have been reported,[6] this was not observed in our study. Furthermore, other small studies have also suggested that RNFL, GCL, and IPL thinning are associated with AMD.[11,12] Variations in findings may be due to pleiotropy and differences in study design. Smaller studies might have false positives and be confounding.

These associations were most pronounced at the L7 and L9 photoreceptor layers at the central macula. Associations at other retinal layers and ETDRS regions were heterogeneous. There are plausible anatomical explanations for this. The retina and choroid are complex 3D structures.[39,40] Photoreceptors are affected in AMD because they are the most metabolically active cells in the human organism and consume the most oxygen per gram of cell.[35] Although photoreceptor loss in advancing age is milder and mainly involves cones, it is worse in AMD, and the number of lost photoreceptors is more localized near the fovea.[35] This explains the associations with the central subfield rather than at greater eccentricity from the fovea. This suggests that these AMD-related SNPs and pathways exhibit topographic selectivity, and associations may be misinterpreted/missed if retinal topographic variation is unaccounted for. This topographic variation may also explain why a previous GWAS on healthy participants did not find significant associations between *CFH* and *ARMS2-HTRA1* with retinal thickness, because macular thickness was defined as the average macular thickness within the ETDRS grid outermost circle of 6 mm.[41] Pleiotropy may also explain why different SNPs are associated with varying effects on the photoreceptor layer thickness. In this regard, aggregating the effects of SNPs using PRS analysis may be advantageous.

Indians demonstrated the thinnest retinal thickness for the same genotype and for the overall PRS_{AMD} compared with the Chinese, particularly in the central subfield, suggesting a greater genetic susceptibility to AMD among the Indians. This is an interesting finding. As the PRS_{AMD} in our study is based on East Asians (mainly Chinese populations), the strong association for photoreceptor layers in the Indians suggests that the transethnic PRS_{AMD} can be applied to other populations. This is also consistent with our previous findings that Indians have the thinnest central subfield and overall macular thicknesses compared with the Chinese and Malays.[42]

The strengths of this study include the use of SNP and PRS_{AMD} analyses to identify associations and their 3D topography. This study is also based on large population datasets that confer statistical power. The limitations include the use of weights for the PRS_{AMD} analyses of the Malay and Indian populations that were obtained from the GAMA GWAS studies of East Asian populations. The R^2 of transethnic PRS for AMD may be deflated due to allele frequencies, LD, and/or environment between the 2 populations.[43] Thus, further studies using population-specific or multipopulation PRS might be ideal for Indian and Malay populations, and the susceptible genetic variants for AMD in those populations should also be included.

In conclusion, the overall genetic susceptibility to AMD and aggregate effects of the complement cascade and lipoprotein metabolism pathway are associated most significantly with L7 and L9 photoreceptor thinning at the central macula in healthy individuals. These structural changes occur at the macula even before AMD onset, suggesting that the photoreceptor layer thickness can serve as an early biomarker for AMD, and topographic variation should be considered.

Footnotes and Disclosures

Originally received: February 9, 2023.
Final revision: July 12, 2023.
Accepted: August 30, 2023.
Available online: September 12, 2023. Manuscript no. XOPS-D-23-00033.

[1] Singapore Eye Research Institute, Singapore National Eye Centre, Singapore, Singapore.

[2] Ophthalmology & Visual Sciences Academic Clinical Program (Eye ACP), Duke-NUS Medical School, Singapore, Singapore.

[3] Department of Ophthalmology, Yong Loo Lin School of Medicine, National University of Singapore, Singapore, Singapore.

[4] Tsinghua Medicine, Tsinghua University, Beijing, China.

[5] Centre for Quantitative Medicine, Duke-NUS Medical School, Singapore, Singapore.

Disclosure(s):

All authors have completed and submitted the ICMJE disclosures form.

The authors made the following disclosures:

Supported by Duke/Duke-NUS Research Collaborations grant: Duke/Duke-NUS/RECA(Pilot)2016/0020, Biomedical Research Council Singapore grant: SPF2014/002, National Medical Research Council Open Fund Large Collaborative Grant: NMRC/LCG/004/2018, NMRC/CG-INCEPTOR/Pre-Clinical Core Platform/2017_SERI, and the National Medical Research Council Clinician Scientist Individual Research Grants: MOE R-317-000-138-115, and NMRC/CIRG/1488/2018.

HUMAN SUBJECTS: Human subjects were included in this study. The study adhered to the tenets of the Declaration of Helsinki. Ethics approval was obtained from the Institutional Review Board of the Singapore Eye Research Institute. Written informed consent was obtained from all participants. No animals were used in this study.

Author Contributions:

Conception and design: Li, Tham, Teo, Tan, Schmetterer, Wong, Cheung, Cheng, Fan

Data Collection: Cheong, Li, Tham, Teo, Tan, Schmetterer, Wong, Cheung, Cheng, Fan

Analysis and interpretation: Cheong, Li, Tham, Teo, Tan, Schmetterer, Wong, Cheung, Cheng, Fan

Obtained funding: N/A

Overall responsibility: Cheong, Li, Tham, Teo, Tan, Schmetterer, Wong, Cheung, Cheng, Fan

Abbreviations and Acronyms:
AMD = age-related macular degeneration; **GAMA** = Genetics of AMD in Asians; **GCL** = ganglion cell layer; **GWAS** = genome-wide association study; **IPL** = inner plexiform layer; **L** = layer; **LD** = linkage disequilibrium; **PRSAMD** = age-related macular degeneration polygenic risk score; **RNFL** = retinal nerve fiber layer; **RPE** = retinal pigment epithelium; **SE** = standard error; **SEED** = Singapore Epidemiology of Eye Diseases; **SNP** = single nucleotide polymorphism; **3D** = 3-dimensional.

Keywords:
Age-related macular degeneration, Single nucleotide polymorphism, Polygenic risk score, Retinal thickness, Genetic loci.

Correspondence:
Qiao Fan, PhD, Centre for Quantitative Medicine, Duke-NUS Medical School, Singapore, 8 College Rd, Singapore 169857. E-mail: qiao.fan@duke-nus.edu.sg.

References

1. Wong WL, Su X, Li X, et al. Global prevalence of age-related macular degeneration and disease burden projection for 2020 and 2040: a systematic review and meta-analysis. *Lancet Glob Health*. 2014;2:e106–e116.
2. Jonas JB, Cheung CMG, Panda-Jonas S. Updates on the epidemiology of age-related macular degeneration. *Asia Pac J Ophthalmol (Phila)*. 2017;6:493–497.
3. Klein R, Chou CF, Klein BE, et al. Prevalence of age-related macular degeneration in the US population. *Arch Ophthalmol*. 2011;129:75–80.
4. Brandl C, Brucklmayer C, Gunther F, et al. Retinal layer thicknesses in early age-related macular degeneration: results from the German AugUR Study. *Invest Ophthalmol Vis Sci*. 2019;60:1581–1594.
5. Kaye RA, Patasova K, Patel PJ, et al. Macular thickness varies with age-related macular degeneration genetic risk variants in the UK Biobank Cohort. *Sci Rep*. 2021;11:23255.
6. Zekavat SM, Sekimitsu S, Ye Y, et al. Photoreceptor layer thinning is an early biomarker for age-related macular degeneration: epidemiologic and genetic evidence from UK Biobank OCT data. *Ophthalmology*. 2022;129:694–707.
7. Kauppinen A, Paterno JJ, Salminen A, et al. Inflammation and its role in age-related macular degeneration. *Cell Mol Life Sci*. 2016;73:1765–1786.
8. Nagai N, Minami S, Suzuki M, et al. Macular pigment optical density and photoreceptor outer segment length as predisease biomarkers for age-related macular degeneration. *J Clin Med*. 2020;9:1347.

9. Fritsche LG, Igl W, Bailey JN, et al. A large genome-wide association study of age-related macular degeneration highlights contributions of rare and common variants. *Nat Genet*. 2016;48:134−143.
10. Cheng CY, Yamashiro K, Chen LJ, et al. New loci and coding variants confer risk for age-related macular degeneration in East Asians [published correction appears in Nat Commun. 2015;6:6817]. *Nat Commun*. 2015;6:6063.
11. Borrelli E, Abdelfattah NS, Uji A, et al. Postreceptor neuronal loss in intermediate age-related macular degeneration. *Am J Ophthalmol*. 2017;181:1−11.
12. Zucchiatti I, Parodi MB, Pierro L, et al. Macular ganglion cell complex and retinal nerve fiber layer comparison in different stages of age-related macular degeneration. *Am J Ophthalmol*. 2015;160:602−607.e1.
13. Wells-Gray EM, Choi SS, Bries A, Doble N. Variation in rod and cone density from the fovea to the mid-periphery in healthy human retinas using adaptive optics scanning laser ophthalmoscopy. *Eye (Lond)*. 2016;30:1135−1143.
14. Joachim N, Mitchell P, Burlutsky G, et al. The incidence and progression of age-related macular degeneration over 15 years: the Blue Mountains Eye Study. *Ophthalmology*. 2015;122:2482−2489.
15. Lavanya R, Jeganathan VS, Zheng Y, et al. Methodology of the Singapore Indian Chinese Cohort (SICC) Eye Study: quantifying ethnic variations in the epidemiology of eye diseases in Asians. *Ophthalmic Epidemiol*. 2009;16:325−336.
16. Rosman M, Zheng Y, Wong W, et al. Singapore Malay Eye Study: rationale and methodology of 6-year follow-up study (SiMES-2). *Clin Exp Ophthalmol*. 2012;40:557−568.
17. Sabanayagam C, Yip W, Gupta P, et al. Singapore Indian Eye Study-2: methodology and impact of migration on systemic and eye outcomes. *Clin Exp Ophthalmol*. 2017;45:779−789.
18. Abràmoff MD, Garvin MK, Sonka M. Retinal imaging and image analysis. *IEEE Rev Biomed Eng*. 2010;3:169−208.
19. Li K, Wu X, Chen DZ, Sonka M. Optimal surface segmentation in volumetric images–a graph-theoretic approach. *IEEE Trans Pattern Anal Mach Intell*. 2006;28:119−134.
20. Zhang L, Buitendijk GH, Lee K, et al. Validity of automated choroidal segmentation in SS-OCT and SD-OCT. *Invest Ophthalmol Vis Sci*. 2015;56:3202−3211.
21. Cornes BK, Khor CC, Nongpiur ME, et al. Identification of four novel variants that influence central corneal thickness in multi-ethnic Asian populations [published correction appears in Hum Mol Genet. 2012 Oct 1;21(19):4365]. *Hum Mol Genet*. 2012;21:437−445.
22. Fan Q, Barathi VA, Cheng CY, et al. Genetic variants on chromosome 1q41 influence ocular axial length and high myopia. *PLoS Genet*. 2012;8:e1002753.
23. Delaneau O, Marchini J, Zagury JF. A linear complexity phasing method for thousands of genomes. *Nat Methods*. 2011;9:179−181.
24. 1000 Genomes Project Consortium, Abecasis GR, Altshuler D, et al. A map of human genome variation from population-scale sequencing [published correction appears in Nature. 2011 May 26;473(7348):544. Xue, Yali [added]; Cartwright, Reed A [added]; Altshuler, David L [corrected to Altshuler, David]; Kebbel, Andrew [corrected to Keebler, Jonathan]; Koko-Gonzales, Paula [corrected to Kokko-Gonzales, Paula]; Nickerson, Debbie A [corrected to Nickerson, Debo]. *Nature*. 2010;467:1061−1073.
25. Fuchsberger C, Abecasis GR, Hinds DA. minimac2: faster genotype imputation. *Bioinformatics*. 2015;31:782−784.
26. Wang K, Li M, Hakonarson H. ANNOVAR: functional annotation of genetic variants from high-throughput sequencing data. *Nucleic Acids Res*. 2010;38:e164.
27. Purcell S, Neale B, Todd-Brown K, et al. PLINK: a tool set for whole-genome association and population-based linkage analyses. *Am J Hum Genet*. 2007;81:559−575.
28. Fan Q, Li H, Wang X, et al. Contribution of common and rare variants to Asian neovascular age-related macular degeneration subtypes. *Nat Commun*. 2023;14:5574.
29. Choi SW, O'Reilly PF. PRSice-2: polygenic risk score software for biobank-scale data. *GigaScience*. 2019;8:giz082.
30. Schoeler T, Choi SW, Dudbridge F, et al. Multi-polygenic score approach to identifying individual vulnerabilities associated with the risk of exposure to bullying. *JAMA Psychiatry*. 2019;76:730−738.
31. Willer CJ, Li Y, Abecasis GR. METAL: fast and efficient meta-analysis of genomewide association scans. *Bioinformatics*. 2010;26:2190−2191.
32. Romero-Vazquez S, Llorens V, Soler-Boronat A, et al. Interlink between inflammation and oxidative stress in age-related macular degeneration: role of complement factor H. *Biomedicines*. 2021;9:763.
33. van Leeuwen EM, Emri E, Merle BMJ, et al. A new perspective on lipid research in age-related macular degeneration. *Prog Retin Eye Res*. 2018;67:56−86.
34. Curcio CA. Soft drusen in age-related macular degeneration: biology and targeting via the oil spill strategies. *Invest Ophthalmol Vis Sci*. 2018;59:AMD160−AMD181.
35. Rozing MP, Durhuus JA, Krogh Nielsen M, et al. Age-related macular degeneration: a two-level model hypothesis. *Prog Retin Eye Res*. 2020;76:100825.
36. Brinks J, van Dijk EHC, Klaassen I, et al. Exploring the choroidal vascular labyrinth and its molecular and structural roles in health and disease. *Prog Retin Eye Res*. 2022;87:100994.
37. Zekavat SM, Lu J, Maugeais C, Mazer NA. An in silico model of retinal cholesterol dynamics (RCD model): insights into the pathophysiology of dry AMD. *J Lipid Res*. 2017;58:1325−1337.
38. McHugh KJ, Li D, Wang JC, et al. Computational modeling of retinal hypoxia and photoreceptor degeneration in patients with age-related macular degeneration. *PLoS One*. 2019;14:e0216215.
39. Cheong KX, Teo KYC, Tham YC, et al. Three-dimensional modelling of the choroidal angioarchitecture in a multi-ethnic Asian population. *Sci Rep*. 2022;12:3831.
40. Cheong KX, Lim LW, Li KZ, Tan CS. A novel and faster method of manual grading to measure choroidal thickness using optical coherence tomography. *Eye (Lond)*. 2018;32:433−438.
41. Gao XR, Huang H, Kim H. Genome-wide association analyses identify 139 loci associated with macular thickness in the UK Biobank cohort. *Hum Mol Genet*. 2019;28:1162−1172.
42. Wong KH, Tham YC, Nguyen DQ, et al. Racial differences and determinants of macular thickness profiles in multiethnic Asian population: the Singapore Epidemiology of Eye Diseases Study. *Br J Ophthalmol*. 2019;103:894−899.
43. Choi SW, Mak TS, O'Reilly PF. Tutorial: a guide to performing polygenic risk score analyses. *Nat Protoc*. 2020;15:2759−2772.